Building Integrated Photovoltaic (PV) Systems: Energy Production Modeling in Urban Environment

Benjamin Govehovitch[1], Stéphanie Giroux-Julien[1], Éric Peyrol[2] and Christophe Ménézo[3]

[1] University Claude Bernard Lyon 1, CETHIL UMR CNRS 5008, Villeurbanne (France)

[2] University Claude Bernard Lyon 1, BioDyMIA, Lyon (France)

[3] University Savoie Mont-Blanc, LOCIE UMR CNRS 5271, INES - Le Bourget-du-Lac (France)

Abstract

In the context of urban densification and increased energy consumption, built environment plays an important role by moving from passive to active constructions in terms of energy production, thanks to building integrated photovoltaic (BIPV) systems.

Existing power generation modeling results may differ significantly from actual production. This difference is, partly, due to the non-inclusion of the surrounding environment in the modeling approach. The main goal of this study is to highlight, in the context of integrated power generation, the importance of modeling the interaction between the BIPV and the studied building but also its interaction with the immediate environment and the local climatic conditions.

The simulation results presented in this paper are from the Vauban district in Saint-Denis (Reunion Island) modeling, in the framework of the ORCHIDEE project, which is supported by the French Agency of Energy Management (ADEME).

Keywords: transient energy production, photovoltaic (PV) solar collectors, urban environment, CFD modeling, inter-building effects, microclimate simulation

1. Introduction

In a world of continuous change, energy consumption and population are rapidly increasing. In most countries, the building sector is the major energy consumer and accounts for over 40 % of the world's total primary energy consumption and for 24 % of greenhouse gas emissions (Hegger et al. (2008)). According to the latest urban population estimated by the United Nations, the population of urban areas has been continually increasing in the last few decades: since 2008, city dwellers account for the majority of the world's population, and this trend will continue. Thus, by 2050, 68 % of the world's population is projected to be urban which represents more than 2.5 billion more people living in an urban area.

Combining population and economical growth with energy demand increase whilst limiting the global carbon footprint is then one of the biggest challenges of the 21st century. The building sector could contribute to a sustainable future by turning cities from energy consumers to energy producers. Solar (photovoltaic and thermal) energy has the opportunity to make a major contribution to this transition.

Studies on solar energy production in building sector have been carried out for many years. However, predictive models of energy production consider isolated buildings without considering their urban context. When the urban environment is considered, it is through close mask shadow and ground albedo without any other interaction with the environment. Early studies have shown that the urban environment induces a specific local climate and especially the Urban Heat Island (UHI) effect, which is now well-established (Taha, 1997). More recent studies highlighted the impact of such microclimates on building energy consumption (Kolokotroni et al., (2012)). Regarding radiation potential most studies which are dedicated to solar cadastre focus on roofs, where solar radiation is mostly direct and the surfaces can be considered as horizontal. However in the context of urban densification, it is equally important to take verticality building integration into consideration, as façade/roof ratios are strongly increasing. Considering inter-building effects in terms of heat and mass transfer, especially regarding radiation, is therefore important. Moreover, the operating conditions of solar collectors - that are considered for predictive models - are usually issued from weather stations located outside of cities (typically airport weather stations). All of these hypotheses introduce a bias, especially for solar PV predicted power generation. It is now well-known that the urban climate is specific and that the level of temperature can be 4 °C to 5 °C higher than in non-urban environments. Solar PV generation depends on both the solar radiation and the operating temperature

Selection and/or peer review under responsibility of Scientific Committee
doi:10.18086/eurosun2018.06.06 Available at http://proceedings.ises.org

level. In addition, the higher the temperature, the more premature the ageing and the lower the production yield. Thus, it is essential to take all the phenomena induced by buildings' surroundings into account and to model the local solar resource accordingly, in order to evaluate the feasibility of the system. This represents the ultimate objective which we currently state and present below.

This paper is organized into three parts. Firstly, previous works about solar energy potential at city scale are presented. Secondly, the studied area is described along with the methodology and software used. Finally, the results of the simulations are discussed, as well as future outlooks.

2. Previous works

Since the early 1970s, urban heat island (UHI) has been identified through a confrontation between dense and sparse areas of human life and activities. A large amount of studies have been dedicated to its origin and causes (Oke, 1973; Santamouris et al. (2004)) as well as its assessment in reference to substantial cities under both mild and severe climate. These first studies have raised awareness of the need for taking the surrounding environment of buildings into more precise consideration.

This has led to more recent studies on buildings and district energy consumption (Yang et al. (2012), Kolokotroni et al. (2012)). Indeed, a higher ambient temperature can reduce energy loads in winter. However, the needs of air-conditioning can be dramatically increased by a higher temperature. Kolokotroni et al. (2012) found that the cooling load in London was 25 % higher than in rural environments, whereas the heating load diminished by 22 %.

In the last few years, a focus has been placed on urban districts, not only from the energy consumption perspective but also from the energy production perspective, turning buildings into energy producers and not only energy consumers. Several studies aim to exploit the city solar potential while attempting to bring more accuracy to the evaluation of solar radiation on surfaces. Cheng et al.(2006) and Lobaccaro et al. (2012a, 2012b), highlighted the huge impact of building planning at a district level, but also the envelope of the surrounding buildings and ground radiation characteristics on the PV power generation potential of a building's façade. Redweik et al. (2013) have shown the need to refine the temporal and seasonal analysis. Using a statistical approach, Sarralde et al. (2015) determined that by optimising urban form, the solar irradiation of roofs could be increased by 9 %, while that of façades could increase by up to 45 %. Thus, an accurate assessment of solar energy potential production is important especially for solar PV on both horizontal and vertical urban surfaces. Such an assessment requires consideration of the building within its environment. Indeed, many inter-building effects can occur and influence the operating conditions of solar collectors, such as shading, reflection, wind channeling, etc.

Regarding urban communities, solar cadastres have been in full expansion all over the world since the early 2010s and mainly treat the solar potential concerning the roofs. These solar potentials are often expressed simply in incident solar energy (kWh/m²/year), in photovoltaic power of installation (kWc), in possible annual production (kWh/year), in hours of production to nominal output (h). The relevance of these solar cadastres varies in an important way according to the degree of available and generated information (geographical description, satellite data, digital model 2D or 3D starting from data LiDAR, etc.) as well as the accuracy level of the associated modeling (radiation on horizontal level, taking into account of the slopes, of the masks, estimation of the PV generation starting from the power peak or of a constant ratio of performance, etc.). A very small number of studies are starting to consider the urban microclimate, such as for the town of Vitoria-Gasteiz in Spain. This study evaluates the potential to solar liability and credit (thermal and photovoltaic) starting from a methodology developed by the Technical University of Madrid in the European project POLIS (2012).

3. Study performed

3.1. Modeling tools

Simulating solar irradiation and photovoltaic energy production at city scale is a considerable technological challenge. Freitas et al. (2015) conducted a review of the most popularly used tools. It appears that each of these softwares relies on specific architecture and assumptions. Thus, some software is based on an all-in-one model (buildings and solar radiation are modeled in a single software, like TOWNSCOPE or SOLENE) whereas some others are plug-ins that can be used along with CAD- or GIS-software (like Autodesk ecotect analysis, SOL or v.sun). CAD software present a higher resolution to GIS software but require high computational power at district scale.

In this study the simulations have been performed with the version 4.3 of the software ENVI-met. ENVI-met is a prognostic, three-dimensional, high-resolution microclimate model. The model is specifically designed to simulate the urban climate taking into account all the phenomena specific to this type of environment. In the ENVI-met model these phenomena are categorized into five categories: atmosphere, soil, vegetation, ground and buildings (Bruse and Fleer, 1998).

Starting with ENVI-met 4.0 (2010), an improvement of the reflective shortwave model has been incorporated: the Indexed View Sphere (IVS) model. This model, aims to better evaluate the reflected radiation received by building façades from their surrounding environment. The formalism used in previous versions of ENVI-met has not been changed (eq. 1).

$$Q_{Bldg,in}(x,y,z) = \sigma_{Bldg}(x,y,z) \times Q_{Bldg,swrefl} \qquad \text{(eq. 1)}$$

where $Q_{Bldg,in}$ (W/m²) represents the incoming shortwave radiation and $\sigma_{Bldg,in}$ the Sky View Factor (SVF), $Q_{Bldg,swrefl}$ is defined in (eq. 3). But instead of considering the reflected radiation only from a geometrical point of view, it takes into account the thermal and radiative properties of the material that reflects the shortwave radiation to the considered façade. Thus, the sky view factor is calculated as follows (Bruse, 2015):

$$\sigma_{Bldg}(x,y,z) = \frac{1}{36}\sum_{az=0}^{35}\sum_{h=0}^{8}[sin(10h+5) - sin(10h-5)]\Gamma_{Bldg} \qquad \text{(eq. 2)}$$

where *az* is the azimuth, *h* is the height and Γ_{Bldg} is a binary flag which is 1 if a building was found in the considered facet for reflection and 0 if no building was found. The reflected radiation coming to the façade from another is evaluated as follows:

$$Q_{Bldg,swrefl}(x,y,z) = \frac{1}{36}\sum_{az=0}^{35}\sum_{h=0}^{8}\xi(h,az)Q_{sw,refl}^{out}(h,az) \qquad \text{(eq. 3)}$$

where $Q_{Bldg,swref}$ (W/m²) is the shortwave radiation reflected by the close surrounding. ξ(h, az) is the actual shielding factor.

3.2. Case Studied

This study is carried out in the framework of ORCHIDEE project, which is supported by the French Agency for Environment and Energy Management (ADEME). The aim of the project is to have a better evaluation and modeling of both thermal comfort and energy consumption in the tropical urban environment. A solar potential in terms of energy generation is considered and may influence – and, in turn, be influenced by - both thermal comfort and energy consumption.

The studied area is the Vauban district, located in Saint-Denis, on the Reunion Island (southern hemisphere). Located in the Indian Ocean, the Reunion Island benefits from a tropical climate with a great number of sunshine hours. The Vauban district is mainly residential, with just a few commercial buildings. In particular, residential buildings are mostly apartments, the rest being detached houses. All buildings have a height of about 12 m. An overview of the district is given on Fig. 1.

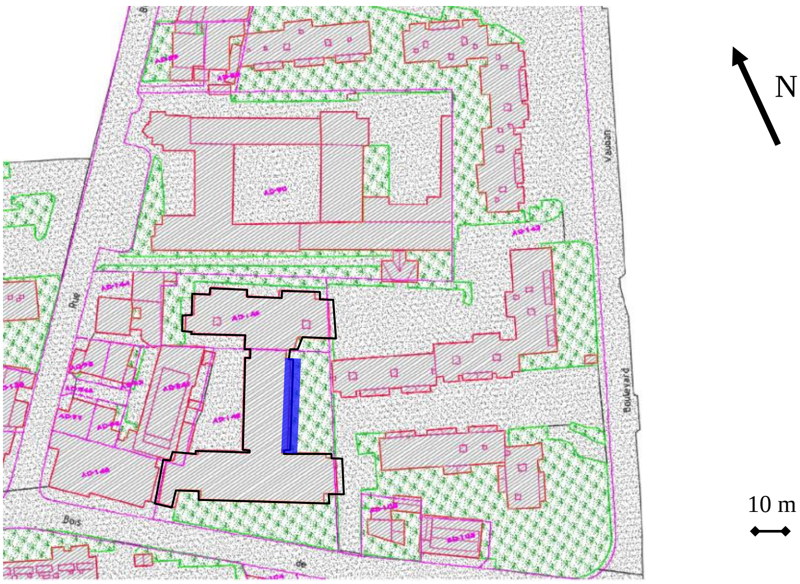

Fig. 1: Overview of the district Vauban

Local climates may vary on the Reunion Island depending on the location but since the Vauban district is located near the coastline, it benefits from annual temperatures roughly between 20 °C and 30 °C. Regarding the solar irradiation, the sunniest period lasts from January to March. February 21st, 2017 has been selected for the study performed (and described later) as it presents the advantages of being one of the sunniest days of the year along with the drawbacks of being the warmest one.

3.3. Input data for the model

The studied day is February 21st, 2017 which was the hottest and one of the sunniest days of that year on the Reunion Island (Tab. 1). This day has been considered to provide with a sufficiently high solar potential for energy production. The weather data used were provided by the nearest meteorological station located in the Saint-Denis airport. Thus, the meteorological conditions are entered in the ENVI-met model (Fig. 2).

Tab. 1: Input configuration data applied in the ENVI-met simulation models

Position Longitude (°) Latitude (°)	55.45 -20.88
Start and duration of the model Date of simulation Start time Total simulation time (h)	02/20/2017 00:00 am 48
Initial meteorological conditions Wind speed measured at 10 m height (m/s) Wind direction (deg) Roughness length at measurement site (m) Specific humidity at calculation domain upper bound (2500 mg/kg) Relative humidity at 2 m height (%)	5.1 45 0.01 17.4 78
Solar radiation and clouds Adjustment factor for solar radiation Cover of low clouds (octas) Cover of medium clouds (octas) Cover of high cloud (octas)	1.0 0.0 0.0 0.0
Soil data Initial temperature in all layers (K) Relative humidity upper layer ([0, -20] cm) Relative humidity middle layer ([-20, -50] cm) Relative humidity deep layer (< -50 cm)	293 50 60 60

The roughness length is the height at which the wind speed theoretically becomes zero. The adjustment factor allows the maximum irradiation value to be set between 500 W/m² (adjustment factor: 0.5) and 1 500 W/m² (adjustment factor: 1.5). The cover of clouds is defined on a scale of 8 values. 0 represents a completely clear sky and 8 represents a fully covered sky.

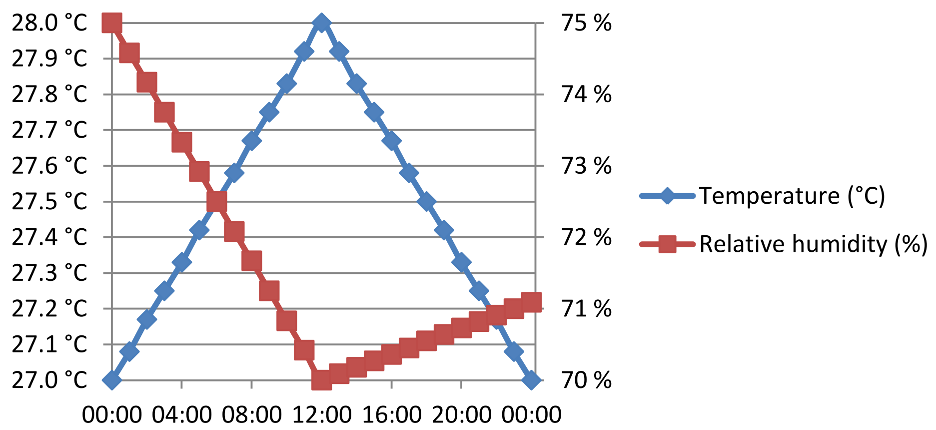

Fig. 2: Evolution of temperature and relative humidity during the day

The presented evolution is quite unusual and does not have a sinusoidal shape but is based on on-field measurements. Note that those measurements are from the nearest weather-station. Unfortunately it could not represent the aforementioned local UHI.

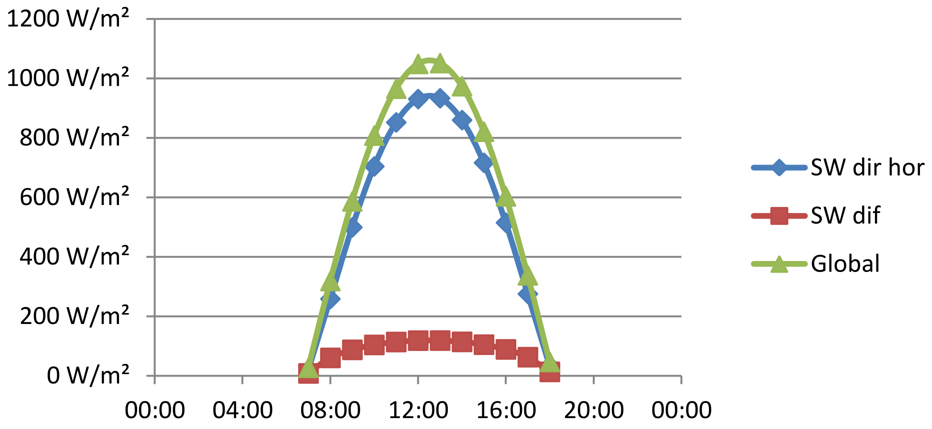

Fig. 3: Evolution of solar radiation density during the day

On Fig. 3, SW dir hor is the shortwave horizontal direct radiation, SW dif is the diffuse shortwave radiation and global is the sum of the two precedents.

The total modeling time was 48 hours. As recommended (Bruse, 2015), the first 24 hours were used to spin up the model in order to get reliable results that would have been influenced by the initialization parameters. Only the last 24 hours were used for the analysis.

3.4. Time and space discretization

The district has been modeled with a 3.6-meter resolution in all directions. This is a compromise between the calculation cost and the necessary resolution to get reliable results. The first 3.6 meters above the ground are subdivided into 5 equal heights. This subdivision is used to attain more reliable results by taking into more precise account the different interrelated physic phenomena near the ground (mass and heat transfers at small scales).

Likewise, the upper bound of the calculation domain (see Fig. 4) was set at twice the height of the highest building in order to avoid any numerical influence of the domain of study (Bruse and Fleer, 1998). At the limit of the domain of study, lateral boundary conditions are set at the default values:

- open for temperature and humidity, which corresponds to a zero deviation,
- forced for turbulence, which means that the values of the 1D model are copied to the border.

Regarding the resolution of the equations, they are discretised at the second order on space and at the first order on time. The results are then averaged on every hour.

3.5. Studied building

The studied building is hatched on Fig. 1. The composition of its walls is described in Tab. 2.

Tab. 2: Composition of studied building walls

Property	Value
Thickness (m)	0.3
Absorption (-)	0.7
Reflection (-)	0.3
Emissivity (-)	0.9
Specific heat (J/K/kg)	840
Thermal conductivity (W/m/K)	0.86

Density (kg/m^3)	930

In order to simplify the simulation, all buildings have the same composition.

Particular focus will be made on the facade outlined in blue on Fig. 1. The interest of this façade lies in the fact it has a direct exposure to sunlight during the first part of the day. However, a small part of the studied wall (16 m high) gets partially shaded by the facing wall (15 m high). Thus, it is possible to evaluate the heterogeneity and time variability of solar irradiation over this façade.

4. Results and discussion

The results presented in this section are issued from simulations run under the version 4.3.2 Summer18 of ENVI-met.

4.1. District irradiance overview

Fig. 1 presents an overview of the irradiance (direct and diffuse) over the studied district. The spatial heterogeneity of irradiance stands out amongst the results. This may have significant influence on the potential of energy production, as will be discussed in the next sections. Roof values are between about 800 and 1 000 W/m² whereas façades values are between 0 and 500 W/m².

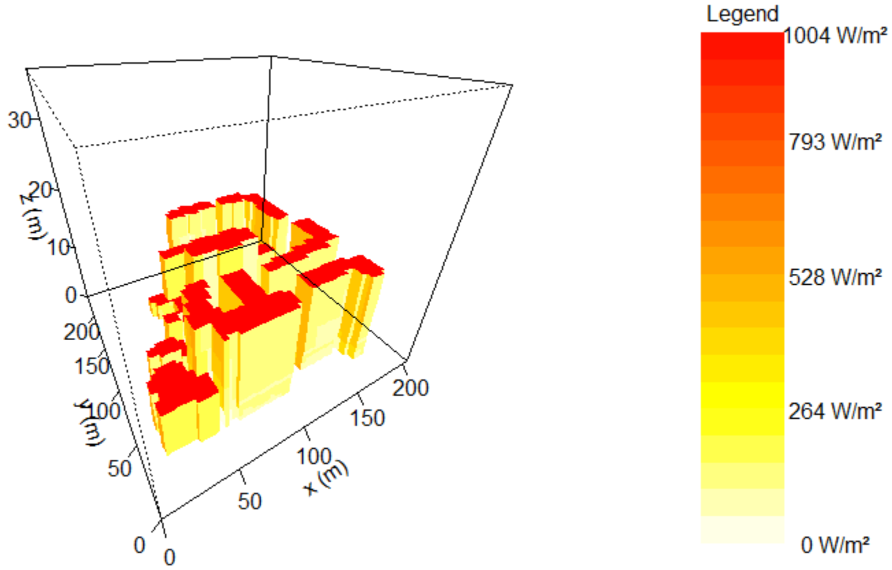

Fig. 4: Domain of study and district irradiance overview on 06/21/2017 at 2:00 pm

4.2. Building surface temperature

In this study, the building surface temperature has been considered to be representative of the BIPV panel. Studying this temperature is important in order to characterize the potential of energy production. Indeed, the higher the PV panel temperature, the lower its efficiency.

As can be seen in Fig. 5, the surface temperature is far from uniform. It presents an important spatial heterogeneity and time variability. Indeed, depending on time or on the façade point, the surface temperature range can exceed 20 °C. It can represent a PV panel's yield loss of almost 10 %.

Regarding the temperature spatial heterogeneity a cooler spot can be observed on the wall. It is due to the drop shadow of the facing building. It highlights the importance of taking into account close environment in predicting energy production.

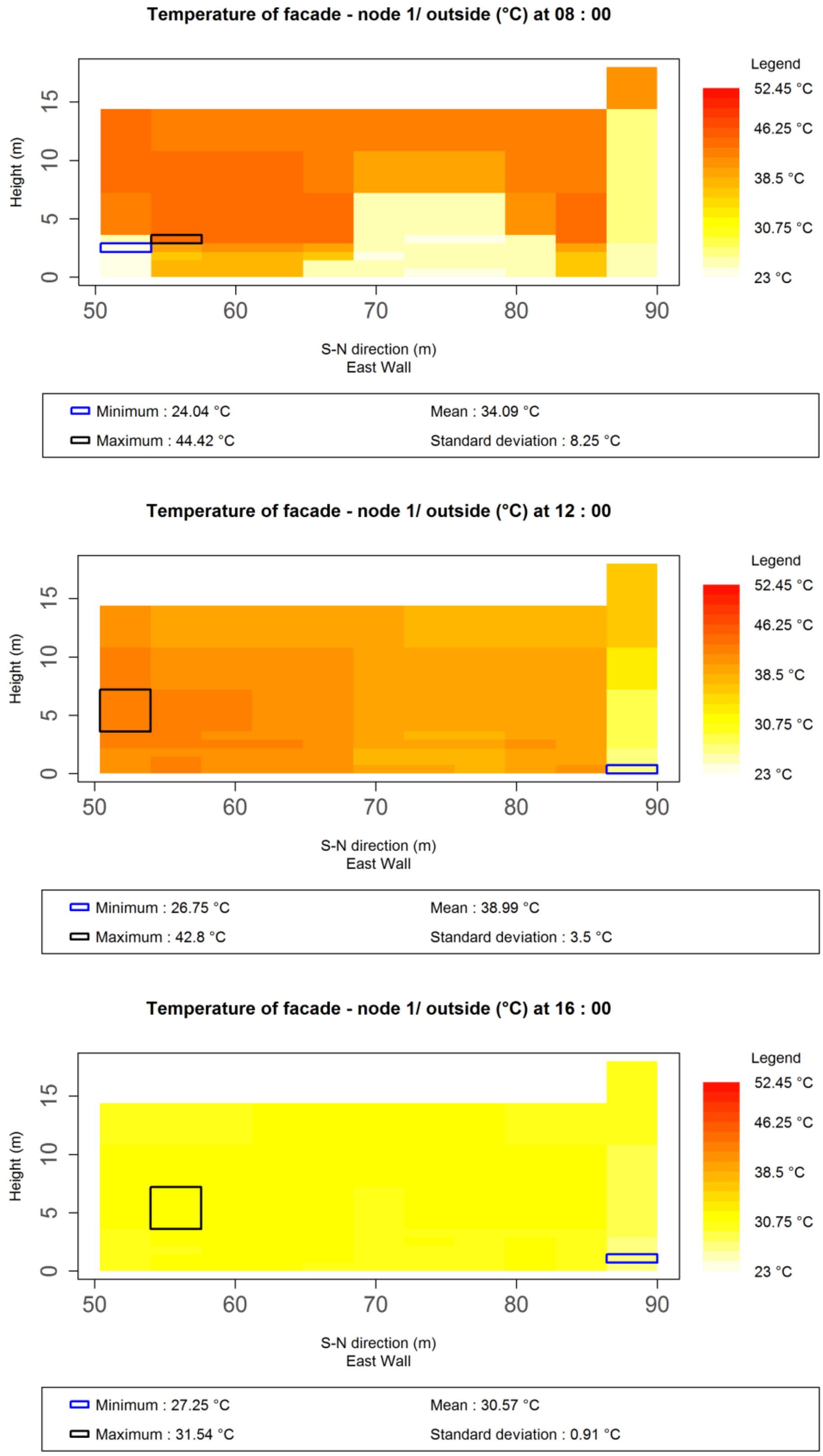

Fig. 5: Evolution of east wall surface temperature during the day

4.3. Shortwave radiation

The results for shortwave irradiance façade map resemble those for surface temperature, as can be seen on Fig. 6. Nonetheless, the spatial heterogeneity is less pronounced. Indeed, vertical heterogeneity is important whereas the horizontal is almost negligible. This result was expected in view of considering mask effects of surrounding buildings.

However, the lighter color spots at 8:00 am reflect the presence of a nearby building that may have a negative impact on potential energy production. Because of the sun spot in the sky, darker grid cells at 4:00 pm are due to pure reflection of diffuse radiation on buildings.

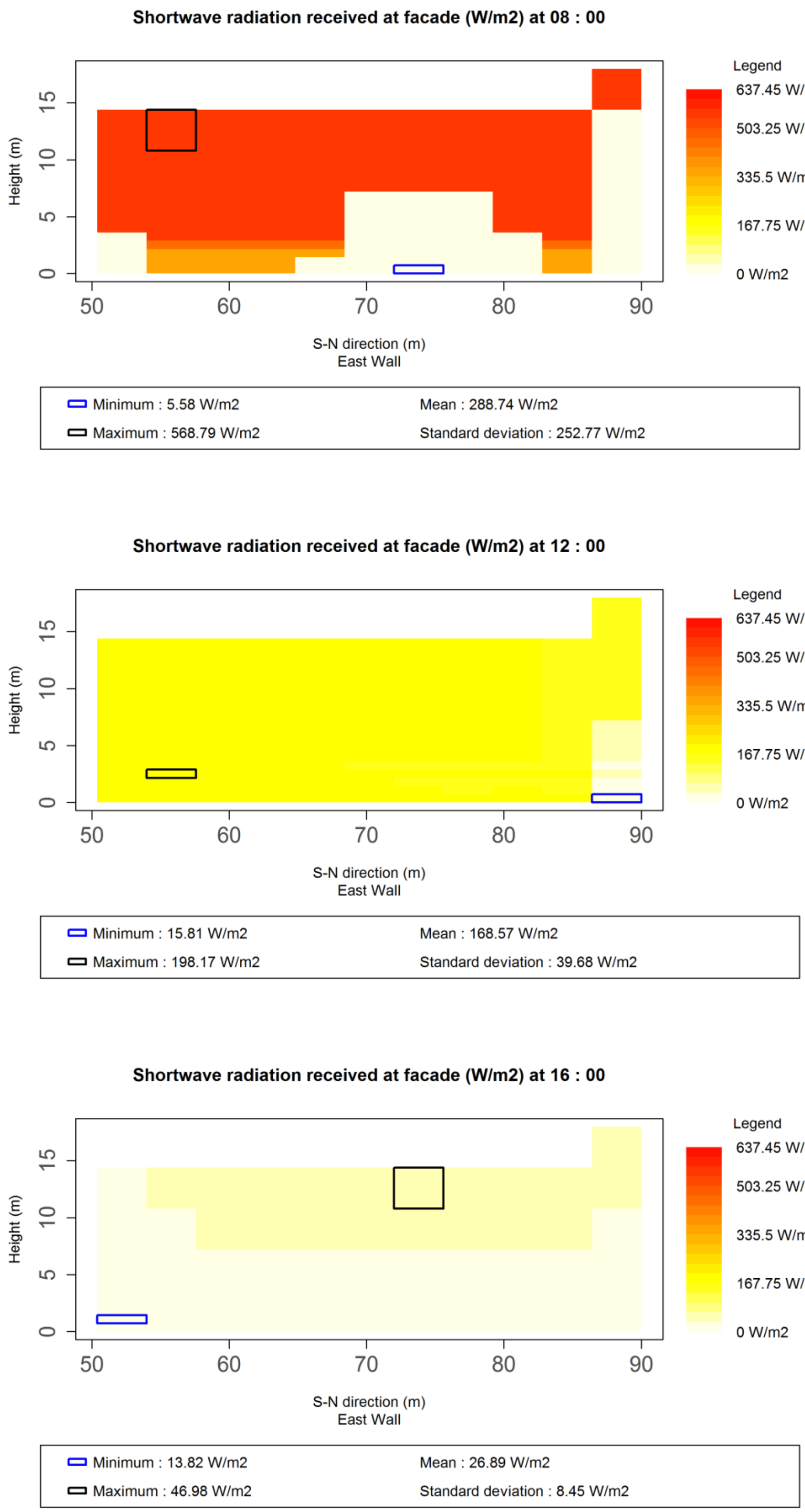

Fig. 6: Evolution of shortwave radiation received at east wall surface during the day

4.4. Integrated solar photovoltaic energy production

A first simple model of photovoltaic energy production has been implemented. A standard photovoltaic panel has been selected. Its technical characteristics are presented in Tab. 4.

Tab. 4: Technical characteristics of the considered photovoltaic panel

Electric characteristics (STC)	Value
Nominal power (P_{nom})	280 Wp
Voltage at nominal power	31.3 V
Current at nominal power	9 A
Temperature coefficient (γ)	-0.42 %/°C

STC: Standard Test Conditions, i.e. irradiance at module level 1000 W/m², spectrum AM1.5 and cell temperature 25°C

The predictive energy production model is based on a strong assumption. Indeed, every cell of the modeled area represents a PV panel which operates at the maximum power point all the time. We then consider power generation right after inverters that are considered to be perfect and by neglecting other PV system loss.

As can be seen on Fig. 7, the power output is mainly influenced by the shortwave radiation received at the façade.

The equation 4 gives the output power as a function of temperature and solar irradiation.

$$P_{out} = \min \left(P_{nom} \times \frac{G}{G_{ref}} \times \left(1 + \gamma \times \left(T - T_{ref}\right)\right), P_{nom}\right) \qquad \text{(eq. 4)}$$

where P_{out} (W/m²) is the output power of the PV panel, P_{nom} (W) the nominal output power of the PV panel, G (W/m²) the irradiance, T (°C) the temperature, γ (%/°C) the temperature coefficient of P_{max} (STC) and the subscript *ref* represents the reference conditions (here STC).

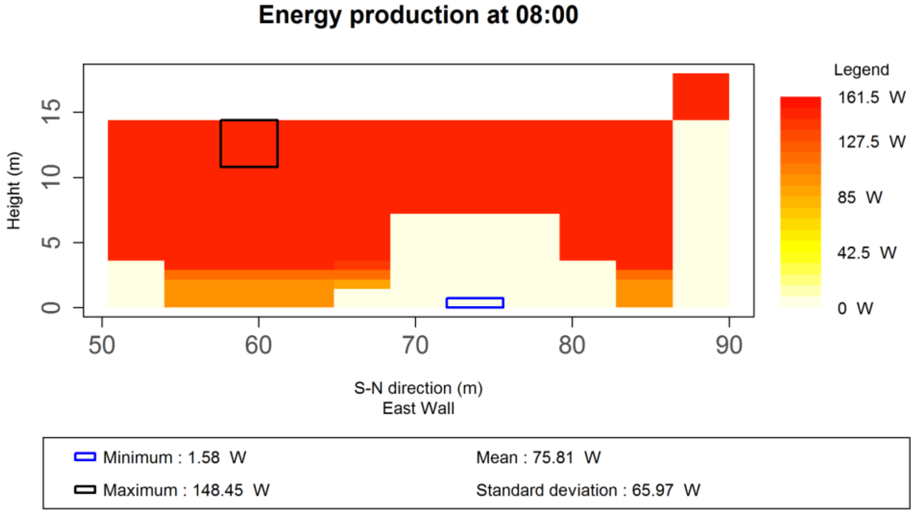

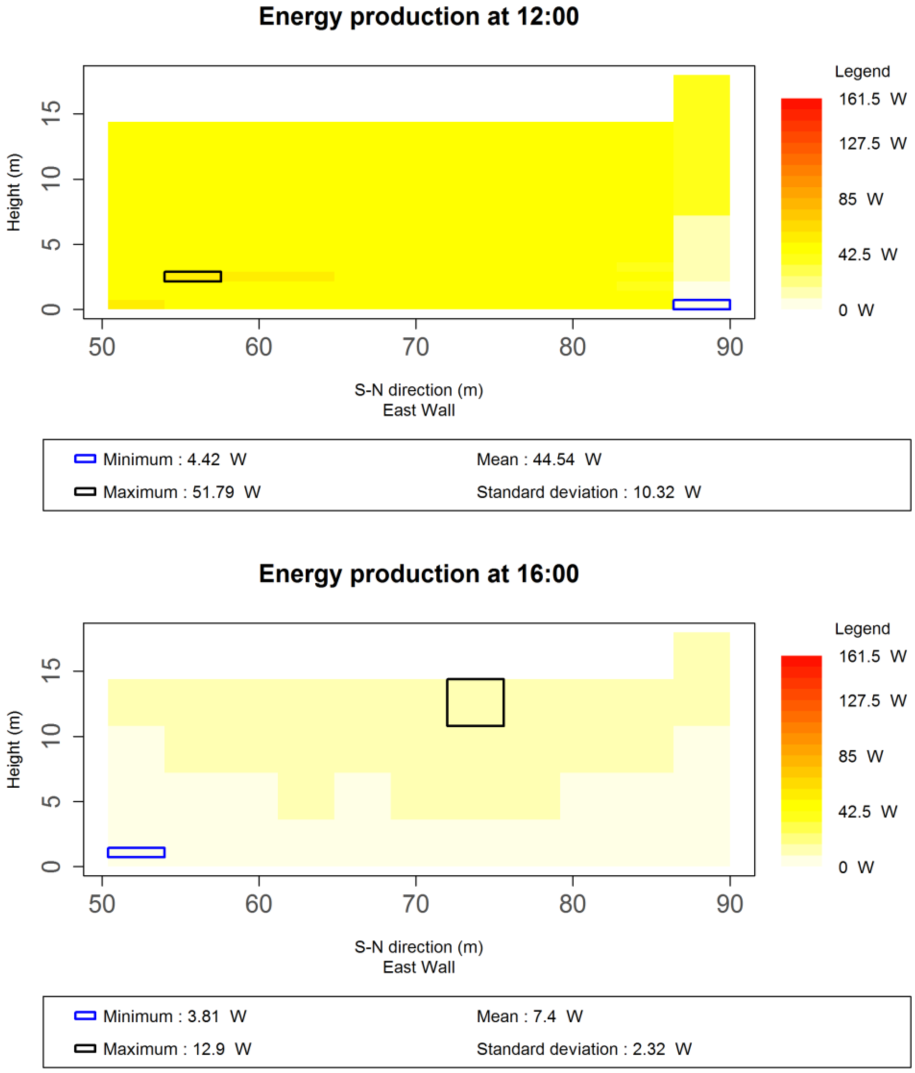

Fig. 7: Evolution of energy production on east wall surface during the day

In order to highlight the importance of taking radiative properties and incident radiation contribution of surrounding buildings into consideration, a simulation has been run while considering those buildings only as masks. The results are presented in Fig. 8.

It can be noticed that there is locally a maximum discrepancy of 19.7 W/m² for shortwave radiation and of local surface temperature of 7 °C. This clearly highlights the impact of inter-building effects especially regarding longwave radiation that induces these important PV surface temperature discrepancies. This induces a power generation discrepancy of 5 W (on nominal power of a PV panel) corresponding to a decrease of 7 % of local power generation, at mean operating conditions for this location.

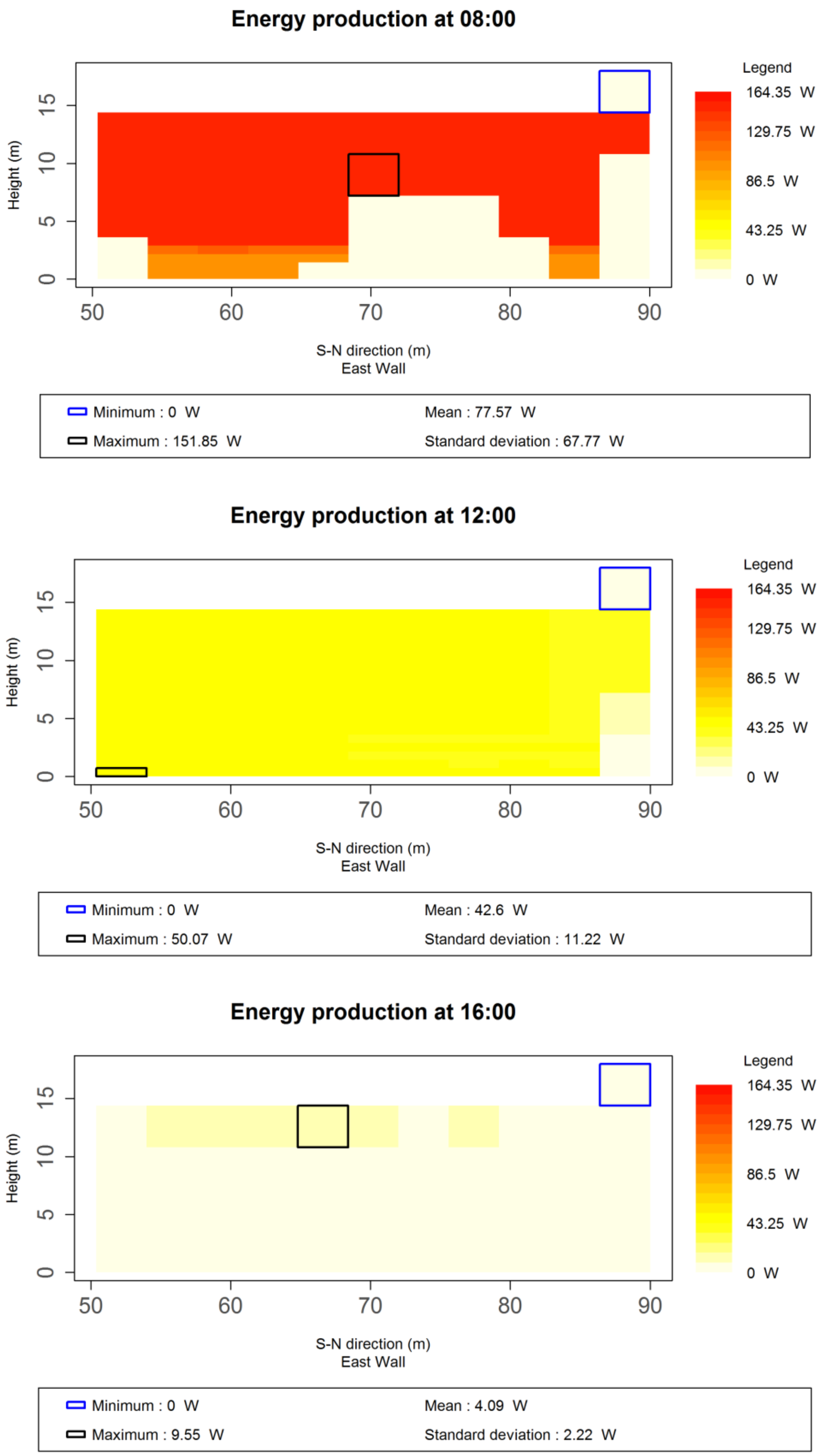

Fig. 8: Evolution of energy production on east wall surface during the day, considering surrounding only as masks

5. Conclusion

Local solar energy production at the district scale is a promising contribution toward satisfying increasing global energy demand. Thus, accurate assessment of energy production potential is critical.

As demonstrated in this paper, taking into consideration the close surrounding of buildings has an important influence on the evaluation of their solar energy production potential. So far, models of energy production only consider close buildings as masks. However, according to the simple production model presented in this paper, it may lead to a bias in the estimation of potential power generation, up to 7 % for a single PV panel. Nonetheless, this study still needs to be spatially expanded to a whole building and even up to an entire district and temporally to the different characteristics of other days of the year. Moreover these differences would have been greater if the local micro-climate had not been considered especially in terms of temperature. They will undoubtedly be more important when we refine the building façades' composition and the PV generation models in future studies. Future works will also involve a validation and a complexification of the proposed energy production model.

Acknowledgements

We would like to acknowledge the Energy and Environment Management Agency (ADEME) for funding the ORCHIDEE project (ADEME 1604C0035).

References

Bruse, M., Fleer, H., 1998. Simulating surface–plant–air interactions inside urban environments with a three dimensional numerical model, Environmental Modelling & Software. 13, 373-384. 10.1016/S1364-8152(98)00042-5

Cheng V., Steemer, K., Montavon M., Compagnon R., 2006. The 23rd Conference on Passive and Low Energy Architecture.

Freitas S., Catita C., Redweik P., Brito M.C., 2015. Modelling solar potential in the urban environment: State-of-the-art review Renewable and Sustainable Energy Reviews. 41, 915-931. 10.1016/j.rser.2014.08.060

Hegger M., Fuchs M., Stark T., Zeumer M., 2008. Energy Manual. Sustainable architecture. Birkhäuser – Edition Detail, Basel.

Kolokotroni M., Ren X., Davies M., Mavrogianni A., 2012. London's urban heat island : Impact on current and future energy consumption in office buildings. Energy and Buildings. 47, 302-311. 10.1016/j.enbuild.2011.12.019

Lobaccaro G., Fiorito F., Masera G., Poli T., 2012. District geometry simulation: a study for the optimization of solar façades in urban canopy layers. Energy Procedia. 30, 1163-1172. 10.1016/j.egypro.2012.11.129

Lobaccaro G., Frontini F., Masera G., Poli T., 2012. SolarPW: A new solar design tool to exploit solar potential in existing urban areas. Energy Procedia. 30, 1173-1183. 10.1016/j.egypro.2012.11.130

Oke T. R., 1973. City Size and the Urban Heat Island. Atmospheric Environment Pergamon Press. 7, 769-779. 10.1016/0004-6981(73)90140-6

Redweik P., C. Catita C., Brito M. 2013. Solar energy potential on roofs and facades in an urban landscape. Solar Energy 97. 332–341. 10.1016/j.solener.2013.08.036

Santamouris M., Adnot J., Alvarez S., Klitsikas N., Orphelin M., Lopes C., Sanchez F., 2004. Cooling the Cities, Presses de l'École des mines de Paris.

Sarralde J. J., Quinn D. J., Wiesmann D., Steemers K., 2015. Solar energy and urban morphology: Scenarios for increasing the renewable energy potential of neighbourhoods in London. Renewable Energy. 73, 10-17. 10.1016/j.renene.2014.06.028

Taha, H., 1997. Urban climates and heat islands: albedo, evapotranspiration and anthropogenic heat. Energy and Buildings. 25, 99–103. 10.1016/S0378-7788(96)00999-1

Yang X., Zhao L., Bruse M., Meng Q., 2012. An integrated simulation method for building energy performance assessment in urban environments Energy and Buildings. 54, 243-251. 10.1016/j.enbuild.2012.07.042

Web references:

Bruse, M., 2015. ENVI-met 4: A Microscale Urban Climate Model. http://envi-met.info – last accessed: 07/26/2018

POLIS Methodology for the Identification of the Detailed Solar Potential of Urban Areas. http://www.polis-solar.eu/IMG/pdf/tool_box_methodologydetailedsolarpotential.pdf - last accessed 08/20/2018

World Urbanization Prospects: The 2018 Revision, 2018. United Nations. https://esa.un.org/unpd/wup/Publications/Files/WUP2018-KeyFacts.pdf - last accessed: 07/20/2018.